AMERICAN SOCIETY FOR MICROBIOLOGY | Infection and Immunity®

HOST-ASSOCIATED MICROBIAL COMMUNITIES

Sex Differences in Population Dynamics during Formation of Kidney Bacterial Communities by Uropathogenic *Escherichia coli*

Lisa K. McLellan,[a] Allyssa L. Daugherty,[a] David A. Hunstad[a,b]

[a]Department of Pediatrics, Washington University School of Medicine, St. Louis, Missouri, USA
[b]Department of Molecular Microbiology, Washington University School of Medicine, St. Louis, Missouri, USA

ABSTRACT Uropathogenic *Escherichia coli* (UPEC), the primary etiologic agent of urinary tract infections (UTIs), encounters a restrictive population bottleneck within the female mammalian bladder. Its genetic diversity is restricted during establishment of cystitis because successful UPEC must invade superficial bladder epithelial cells prior to forming clonal intracellular bacterial communities (IBCs). In this study, we aimed to understand UPEC population dynamics during ascending pyelonephritis, namely, formation of kidney bacterial communities (KBCs) in the renal tubular lumen and nucleation of renal abscesses. We inoculated the bladders of both male and female C3H/HeN mice, a background which features vesicoureteral reflux; we have previously shown that in this model, males develop severe, high-titer pyelonephritis and renal abscesses much more frequently than females. Mice were infected with 40 isogenic, PCR-tagged ("barcoded") UPEC strains, and tags remaining in bladder and kidneys were ascertained at intervals following infection. In contrast to females, males maintained a majority of strains within both the bladder and kidneys throughout the course of infection, indicating only a modest host-imposed bottleneck on overall population diversity during successful renal infection. Moreover, the diverse population in the infected male kidneys obscured any restrictive bottleneck in the male bladder. Finally, using RNA *in situ* hybridization following mixed infections with isogenic UPEC bearing distinct markers, we found that despite their extracellular location (in the urinary space), KBCs are clonal in origin. This finding indicates that even with bulk reflux of infected bladder urine into the renal pelvis, successful ascension of UPEC to establish the tubular niche is an uncommon event.

KEYWORDS *Escherichia coli*, clonality, pyelonephritis, urinary tract infection

Within the unique environments of the mammalian host, expansion of a few bacteria into a large multicellular community is a complex process in which the bacteria must adapt to local conditions and survive mechanical, immunologic, and other stresses. These host forces may impose narrow bottlenecks in which the founding population undergoes a dramatic reduction in genetic diversity as it circumvents some facet of the host environment. Conversely, in the absence of such a bottleneck, the infecting population retains more genetic diversity, potentially allowing for more biological and phenotypic diversity (e.g., virulence and community behaviors) during infection.

Uropathogenic *Escherichia coli* (UPEC), the primary etiologic agent of urinary tract infections (UTIs), encounters such a restrictive population bottleneck as it establishes clonal, biofilm-like intracellular bacterial communities (IBCs) within the superficial epithelial cells (facet cells) of the bladder (1–6). During this pathogenic process, UPEC first binds these facet cells, and a subset of bacteria are then internalized. Within an infected facet cell, a single founder bacterium must avoid expulsion by the cell (7–9) and subsequently replicate in the cytoplasm, ultimately giving rise to a clonal IBC (1–3,

Citation McLellan LK, Daugherty AL, Hunstad DA. 2021. Sex differences in population dynamics during formation of kidney bacterial communities by uropathogenic *Escherichia coli*. Infect Immun 89:e00716-20. https://doi.org/10.1128/IAI.00716-20.

Editor Manuela Raffatellu, University of California San Diego School of Medicine

Address correspondence to David A. Hunstad, dhunstad@wustl.edu.

Received 16 November 2020
Returned for modification 21 December 2020
Accepted 11 January 2021
Accepted manuscript posted online 19 January 2021
Published 17 March 2021

10). Indeed, a UPEC inoculum of 10^7 CFU during experimental cystitis in C3H/HeN and C57BL/6 female mice results in the formation of, on average, ~40 to 100 IBCs (1, 10–14). Bacteria within the IBCs are protected from host defenses and antibiotic treatment, while those remaining in the bladder lumen are susceptible to neutrophil attack and to elimination via micturition (15–18). Bacteria within IBCs later reemerge to infect naive cells, initiating subsequent rounds of IBC formation (15, 19, 20). Thus, the infecting population becomes dominated by founder clones that successfully completed the IBC cycle (1, 10, 19).

Bacteria in the bladder lumen may also ascend the ureters to establish infection in the kidneys (pyelonephritis). Colonization of the kidney represents another event in which a population bottleneck might occur. While cystitis is clinically quite common (annual incidence of community-acquired cystitis is 3 to 13% in females and 0.5 to 3% in males), only ~1% of cystitis cases progress to pyelonephritis, which carries risks for hospitalization, sepsis, and renal abscess formation (21). In fact, 10 to 30% of pyelonephritis cases result in hospital admission, conferring $2 billion to $4 billion in medical costs in the United States annually (21). A common risk factor (primarily in childhood) for developing pyelonephritis is vesicoureteral reflux (VUR), identified in 30 to 45% of young children who present with febrile UTI (22–25). Pyelonephritis in children increases risk for renal scarring and associated lifelong morbidities such as hypertension and end-stage renal disease (24, 26, 27), making it important to understand the pathophysiology and dynamics of upper tract UTI.

The mouse is a highly suitable model for the study of UTI; however, preclinical modeling of UTIs has been performed almost exclusively with female mice, which in most backgrounds resolve upper tract UTI without antibiotic treatment (28, 29). As a result, our molecular understanding of UPEC pathogenesis arises mostly from studies of the female bladder, while mechanisms of UPEC colonization of the kidneys remain a fertile area of study. More recently, we and others have developed models by which male mice can also undergo bladder inoculation (12, 30). Over a time course after equivalent bladder inoculation, males harbor significantly higher bladder and kidney bacterial loads than do females. Indeed, male C3H/HeN mice (a background with documented VUR [31–34]) uniformly develop severe pyelonephritis and >90% exhibit renal abscesses; these outcomes are observed in >70% of androgenized females (12, 35, 36) but only rarely in naive females. As renal abscesses are being nucleated, tubules are occupied by biofilm-like collections of UPEC, which we termed kidney bacterial communities (KBCs) (35, 37). These intratubular (luminal) UPEC colonies are first visible microscopically 5 days postinfection (dpi); thereafter, UPEC multiply rapidly and attract a robust neutrophil response, yielding fully formed KBCs within early abscesses by 7 dpi (35).

In this study, we employed this murine model and a set of "barcoded" UPEC isolates to interrogate the population dynamics of renal tubular colonization by UPEC. We found that in contrast to the female bladder, which imposes a marked bottleneck related to the requirement for intracellular invasion by UPEC, UTI in male mice features much less stringent restriction of genetic diversity among the infecting population, as measured in both the kidneys and bladder. Despite this overall diversity, we found that individual KBCs were clonal, as revealed by *in situ* hybridization (ISH) after mixed infection with distinctly tagged UPEC strains. These data indicate that while ascension to the kidney does not constrain the bacterial population as a whole, pyelonephritis is initiated by individual bacteria that successfully colonize a group of contiguous nephron segments.

RESULTS

Temporal course of male C3H/HeN kidney bacterial loads. Prior studies have provided snapshots of sex differences in UTI outcomes (12, 35). Further, previous work examining population bottleneck events in experimental UTI was limited to female mice (1). Longitudinal studies of bacterial population events in both male and female

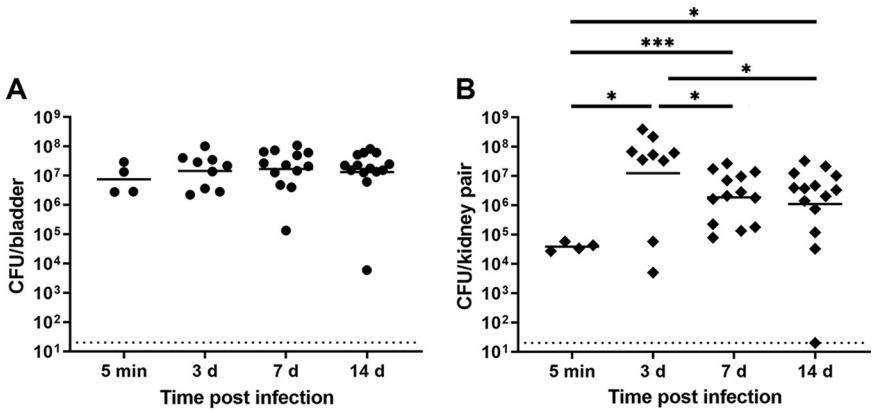

FIG 1 Male C3H/HeN mice develop high-titer cystitis and pyelonephritis. Male C3H/HeN mice were infected with UTI89, and organs were harvested at the indicated intervals. (A) Bladder bacterial loads remained constant across the time points studied. (B) Kidney bacterial loads were statistically highest 3 dpi and then decreased modestly to a stable level at subsequent time points. Horizontal bars indicate geometric means, and the dotted line indicates limit of detection. Data were aggregated from three independent experiments and 4 to 14 mice per group. *, $P < 0.05$; ***, $P < 0.001$.

mice were therefore warranted to better illuminate the dynamics of upper tract UTI. First, we temporally detailed the development of severe pyelonephritis in male C3H/HeN mice, infecting them with UPEC strain UTI89 and measuring organ bacterial loads at different time points postinfection. Bladder bacterial loads were high immediately following inoculation (5 min postinfection [mpi]; geometric mean 7.5×10^6 CFU/bladder) and remained consistent throughout 14 days postinfection (dpi) (Fig. 1A). In contrast, initial kidney titers were substantially lower than bladder titers, with a geometric mean of 3.9×10^4 CFU/kidney pair 5 mpi (Fig. 1B). Kidney titers significantly increased 3 dpi and then decreased modestly (but significantly) to $\sim 10^6$ CFU/kidney pair 7 and 14 dpi (Fig. 1B). On the basis of this pattern, we reasoned that if a bottleneck were present during kidney infection in this model, it was occurring between 3 and 7 dpi (in contrast to the female mouse bladder, in which a marked bottleneck is observed 24 hpi [1]).

Establishment of ascending pyelonephritis in male C3H/HeN mice does not impose a narrow population bottleneck. In mice and in humans with properly functioning vesicoureteral junctions, retrograde flow of urine to the kidneys is precluded, thereby likely restricting the diversity of bacteria that can reach the kidney. In the absence of this anatomic protection (i.e., in C3H/HeN mice and humans with VUR [24, 38]), further bottlenecks might be imposed during colonization of the collecting system and nephron. To investigate this, we infected male C3H/HeN mice with a set of 40 isogenic, PCR-barcoded isolates of UTI89 (1). Additionally, to confirm that the difference between our male data and published female data was not attributable to the mini-surgical inoculation method, we infected a smaller cohort of female C3H/HeN mice using the same technique and studied outcomes at selected time points.

Total organ bacterial loads in males and females were equivalent immediately (5 min) following inoculation (Fig. 2). Of note, organ bacterial loads in males infected with the UTI89-derived strain set (Fig. 2A and B) matched our earlier data with the root strain (Fig. 1), persisting at $\sim 10^6$ CFU at later time points. Meanwhile, organ titers fell in females 7 and 14 dpi (Fig. 2C and D), consistent with prior data (12, 28).

Using multiplex PCR, we assayed the proportion of isolates remaining at each time point, separately interrogating three niches (bladder, left kidney, and right kidney) to determine correlations among the tags detected in these locations. In both females and males, at 5 mpi all tags were detected in the bladder (Fig. 3A and C) and most were detected in the kidneys (Fig. 3B and D). These data indicate that initial ascension to the kidney (e.g., a sex difference in VUR) does not explain the sex differences we have observed in pyelonephritis severity (12, 35).

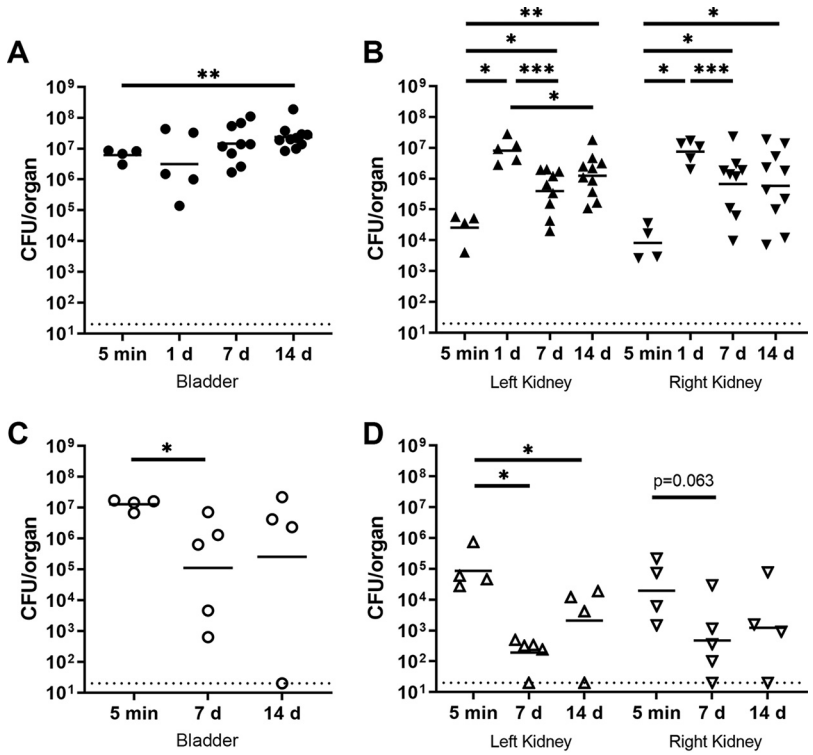

FIG 2 Male C3H/HeN mice maintain higher organ bacterial loads after infection with UTI89-derived barcoded strains than do female mice. C3H/HeN male and female mice were infected with a set of 40 PCR-tagged ("barcoded") isogenic UPEC isolates. At the indicated time points, bacterial loads were determined in homogenates of male bladder (A) and each kidney (B) as well as female bladder (C) and each kidney (D). These results with the isogenic tagged strain set matched those with the root strain UTI89 (from published data and Fig. 1). Data were aggregated from three independent experiments with a total of 4 to 10 mice per condition.

In female mice 1 dpi, the bladder IBC cascade occurs (1, 2, 12, 15) and a significant bladder bottleneck can be discerned; according to published data, 25% of tags remained in the bladder and 60% in the kidneys 1 dpi (1). Despite the fact that this IBC cascade also occurs in the male bladder (12, 15), we observed that in infected male C3H/HeN mice, a majority of isolates (bladder, 94%; kidneys, 97% and 94%) were detected 1 dpi (Fig. 3A and B). At 7 dpi in male C3H mice, we observed a slight narrowing of diversity, with 70%, 74%, and 72% of tags remaining in the bladder and the left and right kidneys, respectively; these proportions were unchanged 14 dpi (Fig. 3A and B). This course aligns temporally with the modest reduction in total kidney bacterial load observed between 3 and 7 dpi (Fig. 1).

In contrast, at 7 dpi in females, a sharp bottleneck was observed in the bladder (48% of tags) and kidneys (23% and 20%, respectively) (all $P < 0.01$ versus males [Fig. 3C and D]). By 14 dpi this bottleneck was even more pronounced (bladder, 36% of tags, $P = 0.05$ versus males; kidneys, 11% and 12%, $P < 0.01$ versus males [Fig. 3C and D]). These data are consistent with those previously reported for females infected via catheter (1). Of note, no significant differences were seen in CFU or tag proportion between left and right kidneys (within one sex) at any time point.

Shared distribution of bacterial clones among urinary tract niches is persistent in males. We next sought to understand whether the same isolates were found within all three niches or if each niche was occupied by a unique set of UPEC clones. Using the multiplex PCR data from male C3H/HeN mice (Fig. 3A and B), we coded each strain and tracked them within each of the studied niches. The proportions of tags common to all three niches were 71%, 88%, 64%, and 58% of isolates at 5 mpi and 1, 7, and 14 dpi, respectively (Fig. 4). The initial rise in shared proportion, followed by a slight

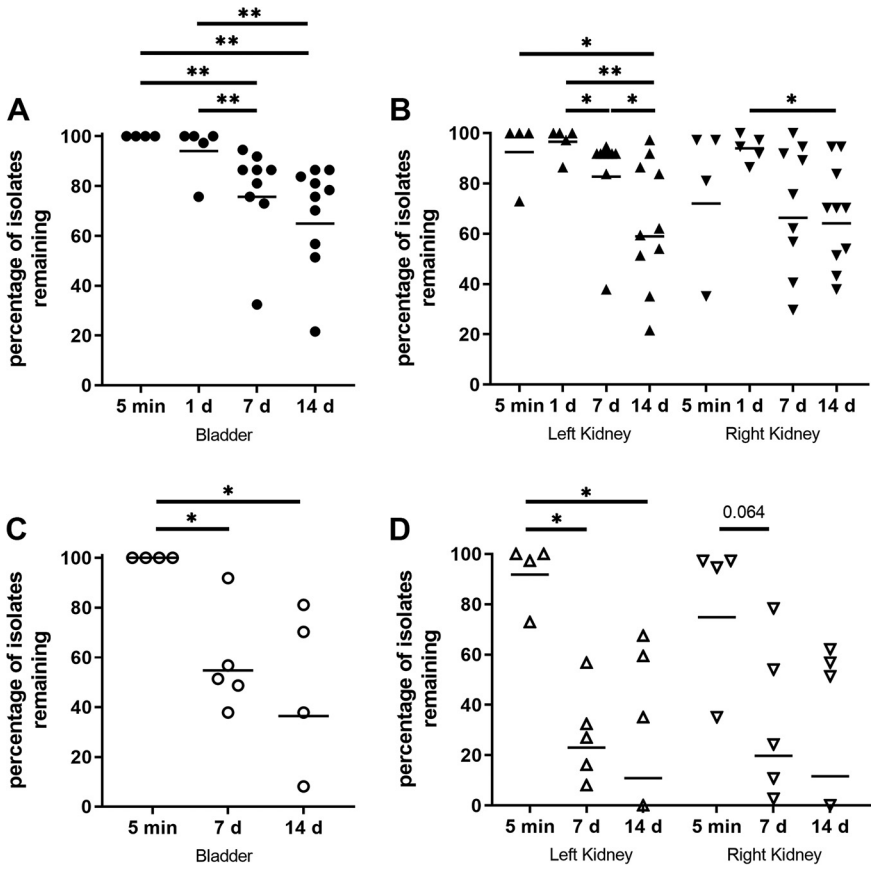

FIG 3 Compared with females, male mice maintain a wide diversity of isolates in the bladder and kidneys. C3H/HeN male or female mice were infected with 40 PCR-tagged (barcoded) isogenic UPEC isolates. Bacterial genomic DNA was extracted from bacterial outgrowths of organ homogenates. Tags remaining in the male bladder (A) and kidneys (B), or female bladder (C) and kidneys (D), were detected by multiplex PCR. Data were aggregated from three independent experiments with a total of 4 to 10 mice per condition. *, $P < 0.05$; **, $P < 0.01$.

narrowing, reflects a mild diversity bottleneck predicted by the overall bacterial loads in the male kidney (Fig. 1) and recapitulates trends in the total number of tags across these time points (Fig. 3A and B).

Meanwhile, a majority of isolates (78%) in female C3H/HeN mice occupied all three niches 5 mpi (Fig. 5A), again indicating that initial ascension to the kidney does not impose a sex-discrepant population bottleneck (see also Fig. 3B and D). However, by 7 and 14 dpi in females, the proportion of isolates common to all three niches had fallen sharply (Fig. 5B and C), in agreement with Fig. 3B and D and earlier work in females (1).

KBCs arise from clonal expansion of founder bacteria within individual tubules. Formation of IBCs in females imposes a bottleneck on bladder population diversity because only a small minority of bacteria successfully complete the IBC cascade; each IBC in this model is formed from a single founder bacterium that has invaded a facet cell (1). While morphological similarities exist between IBCs in the bladder and kidney bacterial communities (KBCs) in the kidney, clonality in the IBCs is thought to arise from prerequisite intracellular invasion (1, 2, 15, 39). This is in contrast to the case with KBCs, which form in the extracellular space (tubular lumen) (35). Therefore, we hypothesized that KBCs would be the product of multiple bacterial clones reaching the tubular lumen. To interrogate the clonal composition of KBCs, we infected C3H/HeN males with a 1:1 mixture of UTI89 HK::Kan^r and UTI89 HK::Chl^r (Fig. 6). We determined the composition of the KBCs 2 weeks postinfection (wpi) by RNA *in situ* hybridization (ISH), detecting expression of Kan^r or Chl^r. Of note, this method was chosen after immunofluorescence microscopy with antibodies against typical protein targets was

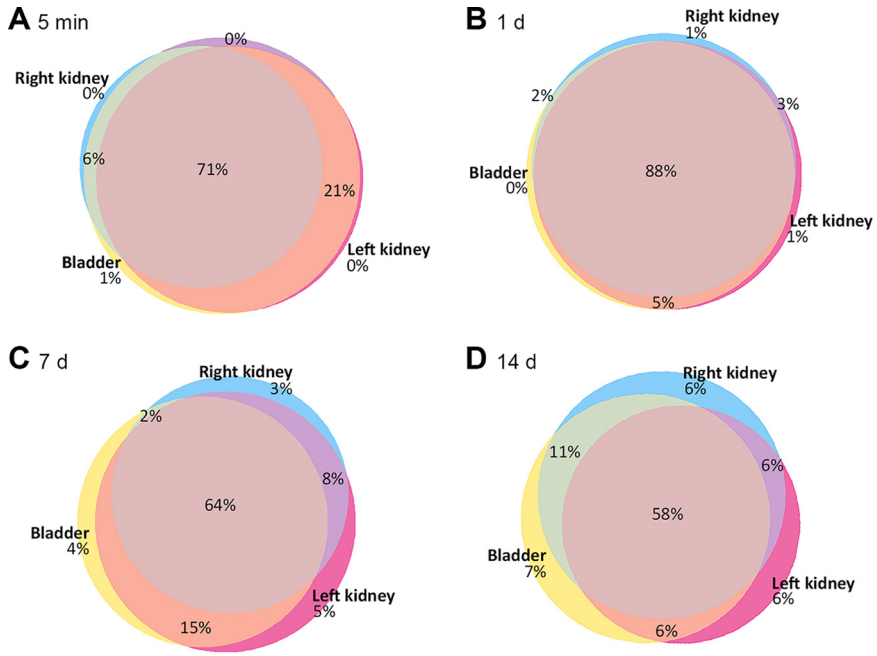

FIG 4 Niche distribution of UPEC in infected male C3H/HeN mice. Using the multiplex PCR data gathered from bladders and kidneys, we quantified the sharing of tags across niches at 5 mpi (A; $n = 4$), 1 dpi (B; $n = 5$), 7 dpi (C; $n = 9$), and 14 dpi (D; $n = 10$). Venn diagrams represent the average proportions of tags detected in the indicated niches. Niche colors: yellow, bladder; hot pink, left kidney; blue, right kidney. Overlap colors: orange, bladder and left kidney; green, bladder and right kidney; purple, left and right kidneys; rose, all three niches. Labels indicate measured proportions in each niche, while colored regions approximate these proportions (smallest regions enlarged for visual clarity). Data were aggregated from three independent experiments, with a total of 4 to 10 mice per condition.

found to be inadequately specific for these experiments. Surprisingly, visualized KBCs were always composed of either UTI89 HK::Kan^r or UTI89 HK::Chl^r but never both (Fig. 6D to F); indeed, of 87 KBCs visualized across 9 mice infected in four independent experiments, 100% were monochromatic. Within an individual kidney section, groups of KBCs formed from a single bacterial strain were located in spatially distinct areas of abscess (Fig. 6D). This finding indicates that at least in this preclinical model of ascending pyelonephritis, the KBC arises from growth and expansion of a founder bacterium that has ascended the nephron to establish a given intratubular focus of infection.

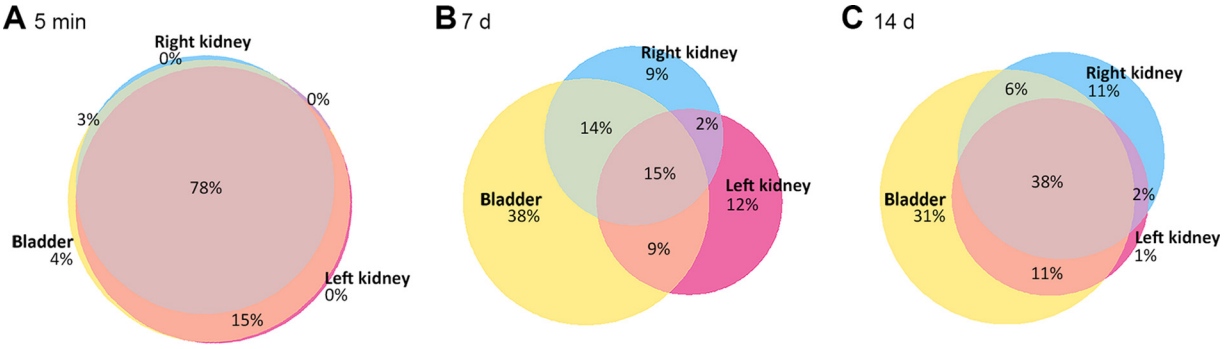

FIG 5 Niche distribution of UPEC in infected female C3H/HeN mice. Using the multiplex PCR data gathered from bladders and kidneys, we quantified the sharing of tags across niches at 5 mpi (A; $n = 4$), 7 dpi (B; $n = 5$), and 14 dpi (C; $n = 4$). Venn diagrams represent the average proportions of tags detected in the various niches. Niche colors: yellow, bladder; hot pink, left kidney; blue, right kidney. Overlap colors: orange, bladder and left kidney; green, bladder and right kidney; purple, left and right kidneys; rose, all three niches. Labels indicate measured proportions in each niche, while colored regions approximate these proportions (smallest regions enlarged for visual clarity). Data reflect one experiment with 4 or 5 mice per group.

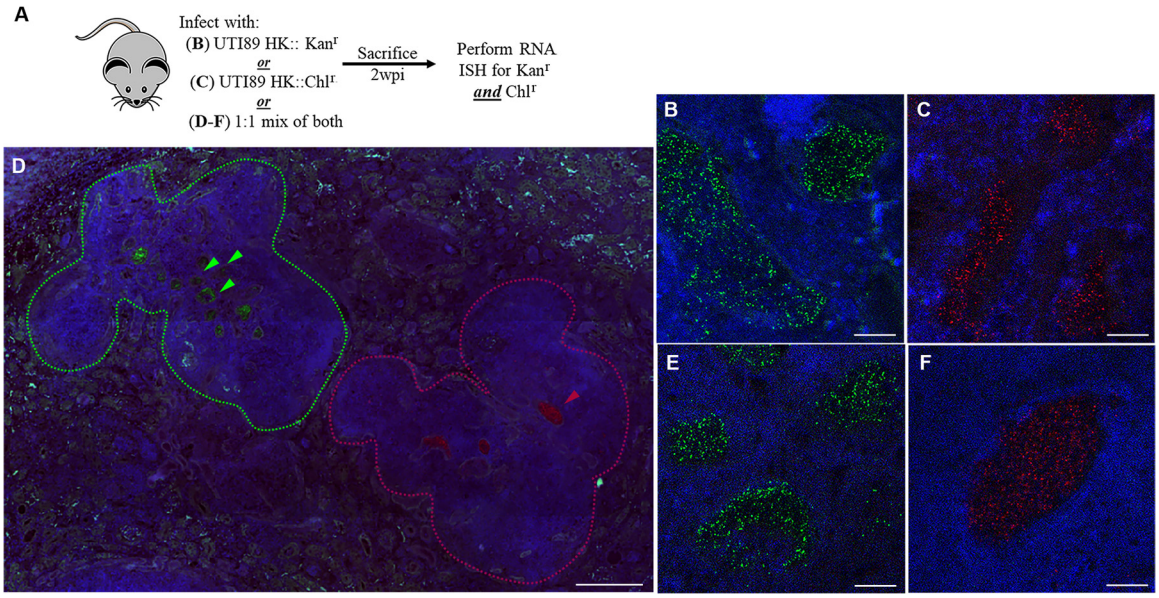

FIG 6 KBCs arise from clonal expansion of individual bacteria. (A) Experimental scheme for inoculation of C3H/HeN male mice with UTI89 HK::Kan^r, UTI89 HK::Chl^r, or an equal mixture of both, followed by KBC examination 2 wpi via RNA ISH and confocal microscopy. (B and C) As controls, mice infected only with UTI89 HK::Kan^r displayed staining only with the Kan^r probe (B; green) and mice infected only with Chl^r displayed staining only with the Chl^r probe (C; red), after both probes were applied to slides. (D) Digitally tiled scans of entire slides after mixed infection revealed Kan^r and Chl^r KBCs within spatially separate areas of abscess in the same kidney; a representative image is shown. Colored arrowheads indicate respectively stained KBCs, and dashed lines demarcate adjacent areas of abscess; scale bar, 200 μm. (E and F) Higher-magnification images of representative KBCs after mixed infection, with staining for either Kan^r (E) or Chl^r (F); no mixed KBCs were seen. Images were selected from 87 analyzed KBCs, collected from 4 independent experiments each with 2 to 9 mice per group; scale bars, 10 μm. Blue stain is for 4′,6-diamidino-2-phenylindole (DAPI) in panels B to F.

DISCUSSION

We conclude that the more robust kidney infection observed in males reflects a greater number of successful founder bacteria (i.e., tagged strains) establishing renal colonization in the male host, despite initial inoculation that is equivalent between sexes. The kidney thus represents a niche, distinct from the bladder tissue, where successful clones can establish themselves and replicate. These kidney-occupying UPEC clones, then, continuously descend from the kidney and contribute to ongoing pathogenesis in the bladder (and, if VUR is present, can likely exchange clones with the contralateral kidney). Moreover, as the kidney maintains a wider diversity of isolates, it is possible for a larger array of phenotypes to be maintained during infection. As a result, UPEC expressing prototypic kidney virulence factors, upon descent into the bladder, might enable additional host-pathogen interactions within the bladder. Finally, as KBCs are clonal, each colonized nephron could act as a unique niche, with bacteria maintaining distinct phenotypes that affect the course or outcome of infection differently than bacteria originating from other reservoirs.

The harboring of a more genetically diverse infection in the kidneys in males —"upstream" of the bladder—thereby overcomes the population bottleneck that would otherwise be evident during initial colonization of the bladder. Meanwhile, the modest narrowing of genetic diversity in the male kidney between 3 and 7 dpi likely reflects a transition from bulk retrograde flow (into the renal pelvis with VUR) to molecular interactions that drive colonization of the nephron (35), potentially coupled with the arrival of phagocytes. In other words, arrival in the kidney in the setting of VUR does not impose a strict bottleneck on the bacterial population, while ascension into the nephron is a comparatively uncommon event accomplished by individual bacteria that express the requisite traits (e.g., for motility or attachment). This model predicts that KBCs are clonal in nature—a conclusion supported by our RNA ISH data. Again,

TABLE 1 Primers used in this study

Set	Primer name	Primer sequence
1	BP 1F	GTACCGCGCTTAAACGTTCAG
	BP 2F	GTACCGCGCTTAAATAGCCTG
	BP 3F	GTACCGCGCTTAAAAGTCTCG
2	BP 4F	GTACCGCGCTTAATAACGTGG
	BP 5F	GTACCGCGCTTAAACTGGTAG
	BP 6F	GTACCGCGCTTAAGCATGTTG
3	BP 7F	GTACCGCGCTTAATGTAACCG
	BP 8F	GTACCGCGCTTAAAATCTCGG
	BP 9F	GTACCGCGCTTAATAGGCAAG
4	BP 10F	GTACCGCGCTTAACAATCGTG
	BP 11F	GTACCGCGCTTAATCAAGACG
	BP 12F	GTACCGCGCTTAACTAGTAGG
5	BP 13F	CTTGCGGCGTATTACGTTCAG
	BP 14F	CTTGCGGCGTATTATAGCCTG
	BP 15F	CTTGCGGCGTATTAAGTCTCG
6	BP 16F	CTTGCGGCGTATTTAACGTGG
	BP 17F	CTTGCGGCGTATTACTGGTAG
	BP 18F	CTTGCGGCGTATTGCATGTTG
7	BP 19F	CTTGCGGCGTATTTGTAACCG
	BP 20F	CTTGCGGCGTATTAATCTCGG
	BP 21F	CTTGCGGCGTATTTAGGCAAG
8	BP 22F	CTTGCGGCGTATTCAATCGTG
	BP 23F	CTTGCGGCGTATTTCAAGACG
	BP 24F	CTTGCGGCGTATTCTAGTAGG

while IBCs in the bladder are clonal due to the process of UPEC internalization into facet cells, we have not observed an intracellular stage associated with KBC formation in our model (1, 35).

KBCs, like IBCs, appear to be biofilm-like in nature (2, 35). However, with respect to various definitions of a biofilm, we have not empirically demonstrated these characteristics (e.g., production of a matrix or differential gene expression in different areas of the bacterial community). Additional definition of KBC characteristics, beyond their clonal nature, may help further illuminate the pathogenic mechanisms important within the kidney.

This work extends our understanding of UPEC population dynamics during UTIs, demonstrating that the susceptible kidney offers a distinct niche for success of bacterial clones and can overcome the bottleneck in genetic diversity that is imposed during establishment of cystitis. Future studies should aim to identify additional molecular determinants of host-pathogen interaction that permit establishment and persistence of upper tract UTI, and how these might relate to ongoing bladder colonization. Specifically, the lack of sharp genetic restriction in the kidney may enable unbiased approaches (e.g., with transposon libraries) to discover kidney-specific UPEC virulence factors.

MATERIALS AND METHODS

Bacterial strains and growth. UPEC strain UTI89 was isolated from a patient with cystitis (10). UTI89 HK::Kan^r and UTI89 HK::Chl^r, as well as a set of 40 isogenic, "barcoded" strains of UTI89 with PCR-detectable tags, were previously published (1). This strain set was generated using the λ Red recombinase system (40). Individual strains were grown statically at 37°C for 18 h in Luria-Bertani (LB) broth and then combined in equal mixture based on optical density at 600 nm (OD_{600}). Bacteria were pelleted at 7,500 $\times$ *g* at 4°C for 10 min and then resuspended to an OD_{600} of 1.0 ($\sim 4 \times 10^8$ CFU/ml) in sterile phosphate-buffered saline (PBS) for inoculation into mice. Type 1 pilus expression was confirmed in all inocula by agglutination of guinea pig erythrocytes (Colorado Serum Company).

Mouse infections. All animal protocols received prior approval from the Institutional Animal Care and Use Committee at Washington University. Male C3H/HeN mice (Envigo) aged 8 to 9 weeks were infected as previously described (12). Briefly, mice were anesthetized with inhaled 3% isoflurane, and the lower abdomen was shaved and sterilized with 2% chlorhexidine solution. A 3-mm midline

abdominal incision was made through the skin and peritoneum, exposing the bladder. The bladder was aseptically emptied before 50 μl of inoculum (1×10^7 to 2×10^7 CFU in PBS) was injected into the bladder lumen via 30-gauge needle over 10 s. The bladder was allowed to expand for an additional 10 s before the needle was removed. The peritoneum and skin incisions were closed with simple, interrupted sutures. At the time of surgery, mice were given sustained-release buprenorphine (1 mg/kg of body weight subcutaneously) for analgesia. At the desired time points, mice were euthanized by CO_2 asphyxiation. Bladders and kidney pairs were sterilely removed and homogenized in 1 ml and 0.8 ml of PBS, respectively. Homogenates were serially diluted and plated on LB agar for CFU enumeration or fixed for histology.

Detection of barcoded UTI89 strains. Methods of detecting the barcoded UTI89 strains have been described previously (1). Briefly, 100 μl of each organ homogenate was spread onto LB agar and incubated overnight at 37°C. To collect genomic DNA, 2 ml of sterile water was added to bacterial lawns and scraped using bent, sterile glass pipettes. Genomic DNA was extracted via the Wizard genomic DNA purification kit (Thermo Fisher); concentration was assayed by NanoDrop (Thermo Fisher), and samples were diluted to 100 ng/μl.

Multiplex PCR was performed using 50 ng of genomic DNA, 1× *Taq* buffer (Invitrogen), 2.5 mM $MgCl_2$, 0.2 mM deoxynucleoside triphosphate (dNTP), 100 pmol each of primers BP-8C (CGTGCCGATC AACGTCTCATTTTCG) and BP-8K (GCTTCAAAAGCGCTCTGAAGTTCCTATAC), 2.5 U of *Taq* DNA polymerase (Invitrogen), and a set of 3 BP-xxF primers (Integrated DNA Technologies) at final concentrations of ~66.6 pmol/primer. Primer sets are shown in Table 1.

PCRs were cycled as follows: (i) initial denaturation of 94°C for 3 min, (ii) 10 cycles of 94°C for 30 s, 62°C for 30 s with a 1°C decrease per cycle, and 72°C for 30 s, (iii) 30 cycles of 94°C for 15 s, 55°C for 15 s, and 72°C for 30 s, and (iv) a final 7-min extension at 72°C. The reaction products were run on 2.5% Tris-borate-EDTA (TBE) agarose gels. The presence or absence of a band representing each individual strain in the multiplex PCR was determined by eye, by a scientist blinded to sample identity. Thirty-seven of the 40 tags were routinely detected in the inoculum (sample gel shown in Fig. S1 in the supplemental material) and were therefore used for all analyses. Ambiguous bands were adjudicated by analysis in an independent multiplex PCR replicate.

Histology and RNA *in situ* hybridization. Infected bladders and kidneys were bisected and fixed in 10% neutral buffered formalin for 24 h. Fixed tissues were embedded in paraffin, sectioned, and processed for RNA *in situ* hybridization (ISH) using protocols and reagents from Advanced Cell Diagnostics (ACD). Specifically, slides were probed with RNAscope probes B-KanR (ACD; catalog number 812371) and B-*E.coli*-CAT-C2 (ACD; catalog number 879281-C2). Detection was then performed using the RNAscope multiplex fluorescent reagent kit v2 (ACD document 323100-USM). Images were acquired on an Olympus FV1200 confocal microscope or with a Zeiss Axio Scan.Z1 digital slide scanner (for digital tiling as indicated).

Statistical analysis. Statistical analysis was performed using Prism (GraphPad Software). Differences were analyzed with the unpaired, two-tailed, nonparametric Mann-Whitney U test. P values of <0.05 were deemed significant. Quantitative Venn diagrams were created using the Eulerr package in R Studio, with circle dimensions adjusted slightly to enable visual display of all niches.

SUPPLEMENTAL MATERIAL

Supplemental material is available online only.

SUPPLEMENTAL FILE 1, PDF file, 0.3 MB.

ACKNOWLEDGMENTS

This work was supported by National Institutes of Health grants R01-DK111541 and R01-DK126697 (to D.A.H.). L.K.M. is supported by a National Science Foundation graduate research fellowship (DGE-1745038) and by the Mr. and Mrs. Spencer T. Olin Fellowship for Women. Confocal microscopy was performed at the Washington University Center for Cellular Imaging (WUCCI), supported by Washington University School of Medicine, the Children's Discovery Institute (CDI-CORE-2015-505 and CDI-CORE-2019-813), and the Barnes-Jewish Hospital Foundation (3770 and 4642).

The 40 isogenic UTI89 isolates were a kind gift from S. J. Hultgren. We thank P. Olson for thoughtful discussions on experimental design and R. McLellan for technical assistance with data analysis.

D.A.H. serves on the Board of Directors for BioVersys AG, Basel, Switzerland. All other authors have no conflicts to declare.

REFERENCES

1. Schwartz DJ, Chen SL, Hultgren SJ, Seed PC. 2011. Population dynamics and niche distribution of uropathogenic *Escherichia coli* during acute and chronic urinary tract infection. Infect Immun 79:4250–4259. https://doi.org/10.1128/IAI.05339-11.
2. Anderson GG, Palermo JJ, Schilling JD, Roth R, Heuser J, Hultgren SJ. 2003. Intracellular bacterial biofilm-like pods in urinary tract infections. Science 301:105–107. https://doi.org/10.1126/science.1084550.
3. Rosen DA, Hooton TM, Stamm WE, Humphrey PA, Hultgren SJ. 2007.

Detection of intracellular bacterial communities in human urinary tract infection. PLoS Med 4:e329. https://doi.org/10.1371/journal.pmed.0040329.
4. Robino L, Scavone P, Araujo L, Algorta G, Zunino P, Vignoli R. 2013. Detection of intracellular bacterial communities in a child with *Escherichia coli* recurrent urinary tract infections. Pathog Dis 68:78–81. https://doi.org/10.1111/2049-632X.12047.
5. Robino L, Scavone P, Araujo L, Algorta G, Zunino P, Pirez MC, Vignoli R. 2014. Intracellular bacteria in the pathogenesis of *Escherichia coli* urinary tract infection in children. Clin Infect Dis 59:e158–e164. https://doi.org/10.1093/cid/ciu634.
6. Flores-Mireles AL, Walker JN, Caparon M, Hultgren SJ. 2015. Urinary tract infections: epidemiology, mechanisms of infection and treatment options. Nat Rev Microbiol 13:269–284. https://doi.org/10.1038/nrmicro3432.
7. Song J, Bishop BL, Li G, Grady R, Stapleton A, Abraham SN. 2009. TLR4-mediated expulsion of bacteria from infected bladder epithelial cells. Proc Natl Acad Sci U S A 106:14966–14971. https://doi.org/10.1073/pnas.0900527106.
8. Miao Y, Li G, Zhang X, Xu H, Abraham SN. 2015. A TRP channel senses lysosome neutralization by pathogens to trigger their expulsion. Cell 161:1306–1319. https://doi.org/10.1016/j.cell.2015.05.009.
9. Miao Y, Wu J, Abraham SN. 2016. Ubiquitination of innate immune regulator TRAF3 orchestrates expulsion of intracellular bacteria by exocyst complex. Immunity 45:94–105. https://doi.org/10.1016/j.immuni.2016.06.023.
10. Wright KJ, Seed PC, Hultgren SJ. 2007. Development of intracellular bacterial communities of uropathogenic *Escherichia coli* depends on type 1 pili. Cell Microbiol 9:2230–2241. https://doi.org/10.1111/j.1462-5822.2007.00952.x.
11. Conover MS, Flores-Mireles AL, Hibbing ME, Dodson K, Hultgren SJ. 2015. Establishment and characterization of UTI and CAUTI in a mouse model. J Vis Exp 2015:e52892. https://doi.org/10.3791/52892.
12. Olson PD, Hruska KA, Hunstad DA. 2016. Androgens enhance male urinary tract infection severity in a new model. J Am Soc Nephrol 27:1625–1634. https://doi.org/10.1681/ASN.2015030327.
13. Cusumano CK, Hung CS, Chen SL, Hultgren SJ. 2010. Virulence plasmid harbored by uropathogenic *Escherichia coli* functions in acute stages of pathogenesis. Infect Immun 78:1457–1467. https://doi.org/10.1128/IAI.01260-09.
14. Rosen DA, Pinkner JS, Jones JM, Walker JN, Clegg S, Hultgren SJ. 2008. Utilization of an intracellular bacterial community pathway in *Klebsiella pneumoniae* urinary tract infection and the effects of FimK on type 1 pilus expression. Infect Immun 76:3337–3345. https://doi.org/10.1128/IAI.00090-08.
15. Justice SS, Hung C, Theriot JA, Fletcher DA, Anderson GG, Footer MJ, Hultgren SJ. 2004. Differentiation and developmental pathways of uropathogenic *Escherichia coli* in urinary tract pathogenesis. Proc Natl Acad Sci U S A 101:1333–1338. https://doi.org/10.1073/pnas.0308125100.
16. Olson PD, Hunstad DA. 2016. Subversion of host innate immunity by uropathogenic *Escherichia coli*. Pathogens 5:2. https://doi.org/10.3390/pathogens5010002.
17. Mulvey MA, Lopez-Boado YS, Wilson CL, Roth R, Parks WC, Heuser J, Hultgren SJ. 1998. Induction and evasion of host defenses by type 1-piliated uropathogenic *Escherichia coli*. Science 282:1494–1497. https://doi.org/10.1126/science.282.5393.1494.
18. Schilling JD, Lorenz RG, Hultgren SJ. 2002. Effect of trimethoprim-sulfamethoxazole on recurrent bacteriuria and bacterial persistence in mice infected with uropathogenic *Escherichia coli*. Infect Immun 70:7042–7049. https://doi.org/10.1128/iai.70.12.7042-7049.2002.
19. Justice SS, Hunstad DA, Seed PC, Hultgren SJ. 2006. Filamentation by *Escherichia coli* subverts innate defenses during urinary tract infection. Proc Natl Acad Sci U S A 103:19884–19889. https://doi.org/10.1073/pnas.0606329104.
20. Mulvey MA, Schilling JD, Hultgren SJ. 2001. Establishment of a persistent *Escherichia coli* reservoir during the acute phase of a bladder infection. Infect Immun 69:4572–4579. https://doi.org/10.1128/IAI.69.7.4572-4579.2001.
21. Foxman B. 2014. Urinary tract infection syndromes: occurrence, recurrence, bacteriology, risk factors, and disease burden. Infect Dis Clin North Am 28:1–13. https://doi.org/10.1016/j.idc.2013.09.003.
22. Hoberman A, Charron M, Hickey RW, Baskin M, Kearney DH, Wald ER. 2003. Imaging studies after a first febrile urinary tract infection in young children. N Engl J Med 348:195–202. https://doi.org/10.1056/NEJMoa021698.
23. Hiraoka M, Hori C, Tsukahara H, Kasuga K, Ishihara Y, Kotsuji F, Mayumi M. 1999. Vesicoureteral reflux in male and female neonates as detected by voiding ultrasonography. Kidney Int 55:1486–1490. https://doi.org/10.1046/j.1523-1755.1999.00380.x.
24. Feld LG, Mattoo TK. 2010. Urinary tract infections and vesicoureteral reflux in infants and children. Pediatr Rev 31:451–463. https://doi.org/10.1542/pir.31-11-451.
25. Hains DS, Schwaderer AL. 2016. Genetic variations in vesicoureteral reflux sequelae. Pathogens 5:14. https://doi.org/10.3390/pathogens5010014.
26. Jacobson SH, Eklöf O, Eriksson CG, Lins LE, Tidgren B, Winberg J. 1989. Development of hypertension and uraemia after pyelonephritis in childhood: 27 year follow up. BMJ 299:703–706. https://doi.org/10.1136/bmj.299.6701.703.
27. Levey AS, Coresh J. 2012. Chronic kidney disease. Lancet 379:165–180. https://doi.org/10.1016/S0140-6736(11)60178-5.
28. Hannan TJ, Mysorekar IU, Hung CS, Isaacson-Schmid ML, Hultgren SJ. 2010. Early severe inflammatory responses to uropathogenic *E. coli* predispose to chronic and recurrent urinary tract infection. PLoS Pathog 6:e1001042. https://doi.org/10.1371/journal.ppat.1001042.
29. Hannan TJ, Hunstad DA. 2016. A murine model for *Escherichia coli* urinary tract infection. Methods Mol Biol 1333:159–175. https://doi.org/10.1007/978-1-4939-2854-5_14.
30. Zychlinsky Scharff A, Rousseau M, Lacerda ML, Canton T, Consiglio CR, Albert ML, Fontes M, Duffy D, Ingersoll MA. 2019. Sex differences in IL-17 contribute to chronicity in male versus female urinary tract infection. JCI Insight 5:e122998.
31. Bowen SE, Watt CL, Murawski IJ, Gupta IR, Abraham SN. 2013. Interplay between vesicoureteric reflux and kidney infection in the development of reflux nephropathy in mice. Dis Model Mech 6:934–941. https://doi.org/10.1242/dmm.011650.
32. Hung CS, Dodson KW, Hultgren SJ. 2009. A murine model of urinary tract infection. Nat Protoc 4:1230–1243. https://doi.org/10.1038/nprot.2009.116.
33. Haraoka M, Hang L, Frendeus B, Godaly G, Burdick M, Strieter R, Svanborg C. 1999. Neutrophil recruitment and resistance to urinary tract infection. J Infect Dis 180:1220–1229. https://doi.org/10.1086/315006.
34. Hopkins WJ, Gendron-Fitzpatrick A, Balish E, Uehling DT. 1998. Time course and host responses to *Escherichia coli* urinary tract infection in genetically distinct mouse strains. Infect Immun 66:2798–2802. https://doi.org/10.1128/IAI.66.6.2798-2802.1998.
35. Olson PD, McLellan LK, Hreha TN, Liu A, Briden KE, Hruska KA, Hunstad DA. 2018. Androgen exposure potentiates formation of intratubular communities and renal abscesses by *Escherichia coli*. Kidney Int 94:502–513. https://doi.org/10.1016/j.kint.2018.04.023.
36. Olson PD, McLellan LK, Liu A, Briden KE, Tiemann KM, Daugherty AL, Hruska KA, Hunstad DA. 2017. Renal scar formation and kidney function following antibiotic-treated murine pyelonephritis. Dis Model Mech 10:1371–1379. https://doi.org/10.1242/dmm.030130.
37. Li B, Haridas B, Jackson AR, Cortado H, Mayne N, Kohnken R, Bolon B, McHugh KM, Schwaderer AL, Spencer JD, Ching CB, Hains DS, Justice SS, Partida-Sanchez S, Becknell B. 2017. Inflammation drives renal scarring in experimental pyelonephritis. Am J Physiol Renal Physiol 312:F43–F53. https://doi.org/10.1152/ajprenal.00471.2016.
38. Lim R. 2009. Vesicoureteral reflux and urinary tract infection: evolving practices and current controversies in pediatric imaging. Am J Roentgenol 192:1197–1208. https://doi.org/10.2214/AJR.08.2187.
39. Justice SS, Lauer SR, Hultgren SJ, Hunstad DA. 2006. Maturation of intracellular *Escherichia coli* communities requires SurA. Infect Immun 74:4793–4800. https://doi.org/10.1128/IAI.00355-06.
40. Datsenko KA, Wanner BL. 2000. One-step inactivation of chromosomal genes in *Escherichia coli* K-12 using PCR products. Proc Natl Acad Sci U S A 97:6640–6645. https://doi.org/10.1073/pnas.120163297.